NANO LETTERS
Cite This: Nano Lett. 2018, 18, 2074−2080
Letter
pubs.acs.org/NanoLett

Composition-Dependent Energy Splitting between Bright and Dark Excitons in Lead Halide Perovskite Nanocrystals

Lan Chen,[†] Bin Li,[†] Chunfeng Zhang,*[,†,‡] Xinyu Huang,[†] Xiaoyong Wang,[†] and Min Xiao*[,†,‡,§]

[†]National Laboratory of Solid State Microstructures, School of Physics & Collaborative Innovation Center of Advanced Microstructures, Nanjing University, Nanjing 210093, China

[‡]Synergetic Innovation Center in Quantum Information and Quantum Physics, University of Science and Technology of China, Hefei, Anhui 230026, China

[§]Department of Physics, University of Arkansas, Fayetteville, Arkansas 72701, United States

Supporting Information

ABSTRACT: Perovskite semiconductor nanocrystals with different compositions have shown promise for applications in light-emitting devices. Dark excitonic states may suppress light emission from such nanocrystals by providing an additional nonradiative recombination channel. Here, we study the composition dependence of dark exciton dynamics in nanocrystals of lead halides by time-resolved photoluminescence spectroscopy at cryogenic temperatures. The presence of a spin-related dark state is revealed by magneto-optical spectroscopy. The energy splitting between bright and dark states is found to be highly sensitive to both halide elements and organic cations, which is explained by considering the effects of size confinement and charge screening, respectively, on the exchange interaction. These findings suggest the possibility of manipulating dark exciton dynamics in perovskite semiconductor nanocrystals by composition engineering, which will be instrumental in the design of highly efficient light-emitting devices.

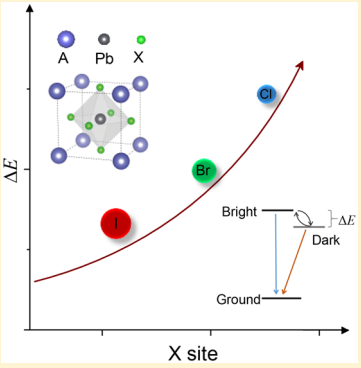

KEYWORDS: *Lead halide perovskite, nanocrystal, dark state, magneto-optical spectroscopy, time-resolved photoluminescence spectroscopy*

The groundbreaking discovery of perovskite solar cells[1−4] has stimulated rapidly growing interest in understanding the optical properties of perovskite semiconductors with various nanostructures. Colloidal nanocrystals of perovskite lead halides have been synthesized with highly efficient photoluminescence (PL) emission, defect tolerance and broad spectral coverage,[5−12] which are promising for applications in optoelectronic devices including light-emitting diodes (LEDs),[1,13−23] lasers,[23−26] and quantum light emitters.[9,27−30] In semiconductor nanocrystals, the excitonic effect controls the light emission properties. Exciton levels with exotic fine structures have recently been found in perovskite semiconductor nanocrystals, which originate from the combined effects of strong spin−orbit coupling, electron−hole exchange interaction, and symmetry distortion.[31−34] Exciton states may be further coupled to free charges, forming trion states.[31,33,34] As well as these emissive transitions, other excitonic states with spin configurations that are optically inaccessible also exist.[34−37] The presence of such dark excitonic states may strongly affect the performances of perovskite nanocrystal devices.[34] Thus, it is of both fundamental importance and technical meaning to investigate the dynamics of dark excitons in perovskite semiconductor nanocrystals.

Another intriguing aspect of perovskite semiconductor nanocrystals is their color tunability. The bandgap of lead halides of the type $APbX_3$ (X = Cl, Br, and I) can be tuned over the whole visible range by simply changing the halide stoichiometry at the X site via cost-effective solution-based approaches.[5,38−42] The optoelectronic properties of $APbX_3$ nanocrystals are also sensitive to the cation at the A site.[43−46] The charge dynamics in perovskite semiconductors with organic cations (i.e., A = methylammonium ($CH_3NH_3^+$, MA^+) or formamidinium ($CH(NH_2)_2^+$, FA^+)) is modified in comparison to that in all inorganic perovskites ($CsPbX_3$) due to the formation of large polaron.[47,48] These merits have stimulated interest in using perovskite nanocrystals with different compositions in LEDs.[1,14−19,22]

In this work, we report the observation of a marked composition dependence of the dark exciton dynamics in perovskite semiconductor nanocrystals. The dark state is manifested with an ultraslow decay component following a dominant subnanosecond faster decay component in the PL decay dynamics at cryogenic temperatures, which is spin related as revealed by magneto-optical spectroscopy. The decay dynamics is understood by a three-level model including a bright excited level and a dark excited level with energy splitting of ΔE. The derived values of ΔE in $CsPbX_3$ nanocrystals decrease monotonically as the X site is substituted with heavier

Received: January 14, 2018
Revised: February 10, 2018
Published: February 21, 2018

DOI: 10.1021/acs.nanolett.8b00184
Nano Lett. 2018, 18, 2074−2080

elements (i.e., Cl → Br → I). This trend is qualitatively explained by consideration of electron−hole interaction in the weak confinement regime. When Cs^+ at A site is replaced by FA^+, ΔE decreases dramatically, which is probably caused by the strong charge screening effect of the organic cations. Our work reports the first observation of composition-dependent energy splitting between bright and dark states in perovskite semiconductor nanocrystals. These findings suggest the possibility of manipulating dark exciton dynamics in perovskite semiconductor nanocrystals by composition engineering, which will be instrumental in the design of highly efficient light-emitting devices.

Nanocrystal samples of perovskite semiconductors are synthesized using wet chemical methods (see the Supporting Information for details).[5,25] We start synthesizing $CsPbBr_3$ nanocrystals, which is further employed as a precursor to prepare $CsPbX_3$ nanocrystals with different halides through anion exchange. This approach can minimize the influence of size difference in nanocrystals with different halides. We have studied five different $CsPbX_3$ samples ($CsPbCl_3$, $CsPbCl_xBr_{3-x}$ ($x \sim 1.5$), $CsPbBr_3$, $CsPbBr_yI_{3-y}$ ($y \sim 1.8$), and $CsPbI_3$) with bandgaps covering the visible range (Figure 1a). The quantum yield of PL emission in these nanocrystals are estimated to be about 15%, 50%, 90%, 90%, and 95%, respectively. The nanocrystals are characterized with pseudocubic structures[25] with an average size L of ≈10 nm as characterized by transmission electron microscopy (TEM) (Figure. 1b). The sample of $FAPbBr_3$ nanocrystals is also prepared with similar size (Figure S1), and the bandgap is comparable to that of the $CsPbBr_3$ nanocrystals (Figure 1c). To study the dark excitonic states, we acquire the time-resolved PL (TRPL) spectra by placing film samples of nanocrystals with a Faraday configuration in the sample chamber of a superconducting magnet. TRPL curves are recorded at the PL peak wavelength by time-correlated single-photon counting using an avalanche photodiode having a temporal resolution of ∼50 ps. The data are recorded with 16 ps per channel.

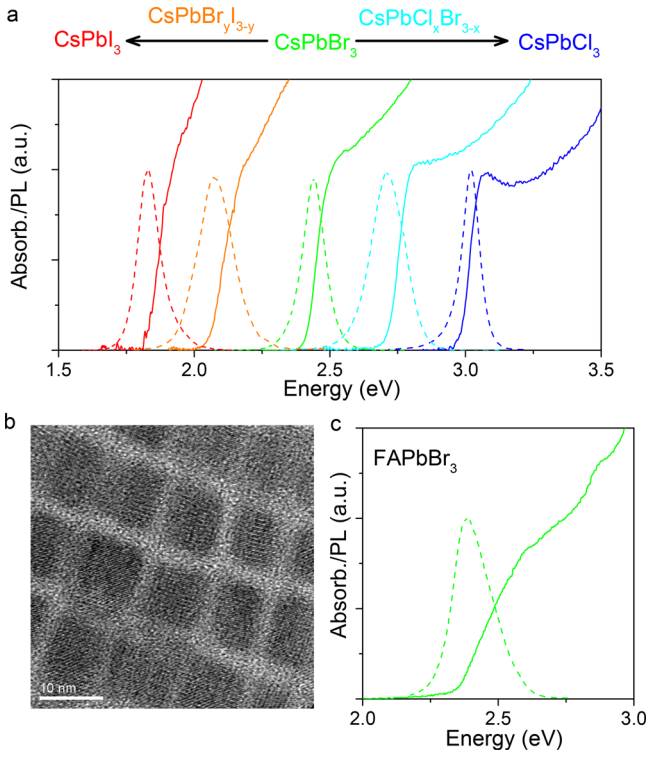

Figure 1. (a) Absorption and PL spectra of $CsPbX_3$ nanocrystals with different anions. Samples were prepared by the anion-exchange approach using precursor $CsPbBr_3$ nanocrystals. (b) TEM image of $CsPbBr_3$ nanocrystals. (c) Absorption and PL spectra of $FAPbBr_3$ nanocrystals.

Figure 2 shows the PL dynamics recorded from $CsPbBr_3$ nanocrystals at different temperatures. PL dynamics strongly depend on temperature (Figure 2a). At 4 K, the TRPL spectrum can be divided into two processes: a dominant fast decay (∼0.7 ns) and a slow decay (∼350 ns). As temperature increases, the slower component gradually becomes more pronounced with decay lifetime shortened. The two components merge at a higher temperature (>70 K), which can be understood as thermal activation-induced mixing of bright and dark excitonic states.[34] The fast component originates from the radiative recombination and energy relaxation of the bright excitons, and the long one is caused by the recombination of the dark excitons (see the inset, Figure 2a).[36,37,49,50] To confirm this assignment, an external magnetic field is applied to manipulate the dark state. If the dark excitonic state is related to spin degree of freedom, it may mix with the bright excitonic state under an applied magnetic field.[34,37,49] Such a magnetic brightening effect is clearly observed (Figure 2b). With an applied magnetic field of 10 T, the amplitude of the slow component increase markedly. These features are characteristic of a spin-forbidden dark exciton state. With increasing temperature, the magnetic field effect becomes less significant (Figure S2) and the contribution of the slow component in total PL emission increases (Figure S3). These results are consistent with the scenario of bright-dark state mixing induced by thermal activation.

In literature, a long-lived decay component in TRPL traces recorded from $CsPbBr_3$ nanocrystals at room temperature was explained by considering the presence of trap states.[51] The process of electron trapping back to the emissive state may induce a slow decay component.[51] We have also observed such a long-lived component at higher temperatures (>150 K, Figure S4). The magnitude of such a long-lived component is strongly dependent on temperature, which becomes nearly undetectable with temperature below 150 K (see the inset of Figure S4). The long-lived component observed at cryogenic temperatures (<50 K) is unlikely to be contributed by such a detrapping effect giving its temperature- and magnetic-field-dependent behaviors. The slow component merges with the fast component with increasing temperature from 4.2 to 70 K, which is a typical behavior of bright- and dark-state mixing.[52] Our assignment of the magnetic-field-dependent behavior to the scenario of bright−dark-state mixing is consistent with the recent magneto-optical experiments on both ensemble[34] and single dot levels.[32] Moreover, such an assignment is further verified by the transient absorption (TA) measurements (Figure S9). Over 20% amplitude ratio of the long-lived component has been observed at 4 K (Figure S9b), which is not distinguishable at room temperature (Figure S9c), indicating that the long-lived component is not mainly caused by the detrapping effect.

For a better understanding the dynamics of dark excitons, we use a three-level model proposed in previous works on CdSe nanocrystals to derive ΔE (see the inset of Figure 2a).[36,37,49,50,53−55] This phenomenological model assumes a bright excitonic state (B) and a dark excitonic state (D) with energy splitting of ΔE that recombine to the ground state (G)

DOI: 10.1021/acs.nanolett.8b00184
Nano Lett. 2018, 18, 2074−2080

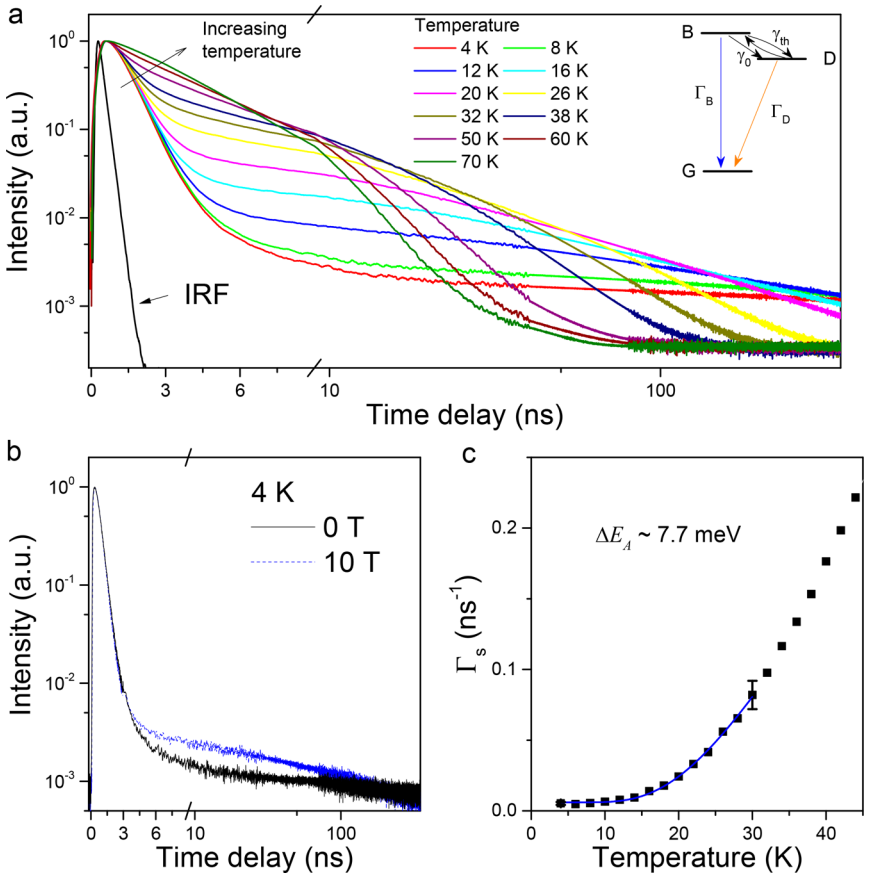

Figure 2. (a) TRPL curves of $CsPbBr_3$ nanocrystals recorded at different temperatures. The instrumental response function (IRF) is included for reference. Insert depicts the three-level model with the ground state (G), bright state (B), and dark state (D). Γ_B and Γ_D are the recombination rates of the bright and dark state. γ_0 is the zero-temperature rate of B → D relaxation. γ_{th} is the thermalization rate caused by the interaction with phonon mode. (b) TRPL curves recorded from $CsPbBr_3$ nanocrystals at 4 K with and without an applied external magnetic field of 10 T, respectively. (c) The temperature-dependent relaxation rate of the slow decay component analyzed with the three-level model. The dashed line is the fitting curve.

with decay rates of Γ_B and Γ_D (including radiative and nonradiative channels), respectively. Assuming that the thermalization of the excitonic states is induced by the interaction with acoustic phonons, the rates for B → D and D → B relaxation processes are $\gamma_0(N_B + 1)$ and $\gamma_0 N_B$, respectively. Here, γ_0 is the B → D relaxation rate at zero temperature and $N_B = 1/[\exp(\Delta E_A/k_B T) - 1]$ is the phonon number at the temperature T of the Bose−Einstein distribution with an activation energy of ΔE_A. In the three-level model, $\Delta E_A = \Delta E$. In previous studies on CdSe nanocrystals, the three-level model was solved by assuming the rate of spin flip $\gamma_0 \gg \Gamma_B$,[50] which may not be valid for perovskite nanocrystals. Instead, the interband recombination is proposed to be tightly associated with the spin flip process due to Rashba effect.[46,56] Considering this effect, we solve the rate equation of the three-level model without the assumption of $\gamma_0 \gg \Gamma_B$ (see the Supporting Information for details). In this case, the decay rate of fast and slow components Γ_f and Γ_s at low temperature can be approximately derived as:

$$\Gamma_f \approx \Gamma_B + \gamma_0(2N_B + 1)$$

$$\Gamma_s \approx \Gamma_D + \Gamma_B\gamma_0 N_B/(\Gamma_B + (2N_B + 1)\gamma_0)$$

Using this model, the value of ΔE can be derived from the temperature-dependent rates of the slow decay component (Figure 2c). Approximately, Γ_D can be taken from the decay curve recorded at 4 K. In $CsPbBr_3$ nanocrystals, ΔE is estimated to be ~7.7 meV, which is of the same order as the values reported for CdSe nanocrystals.[36,37,50] To some extent, the three-level model is oversimplified for accurate evaluation of ΔE because of the complicated structures of excitonic levels in perovskite semiconductor nanocrystals.[57] Nevertheless, the values provide a relative metric for qualitative understanding of the composition dependence of dark exciton dynamics.

Next, we focus on understanding the dark exciton dynamics in perovskite semiconductor nanocrystals with different halides. The bandgaps of $CsPbX_3$ nanocrystals become smaller with heavier halide elements. Figure 3a,b show the TRPL curves recorded from perovskite semiconductor nanocrystals when Br is partially substituted with Cl and I, respectively. The temperature-dependent behaviors are similar to that in $CsPbBr_3$ nanocrystals, with a fast component related to the bright excitonic state and a slow component related to the dark state. Interestingly, both components show significant composition dependences. As the halide becomes heavier, i.e., Cl → Br → I, the decay rate of fast component (Γ_f) gradually becomes slower (Figure 3c), and the slow decay component becomes more important. The derived value of ΔE also strongly depends on the halide. With heavier halides, ΔE is smaller. This is consistent with magneto-optical experiments that magnetic field effect is larger in perovskite semiconductor nanocrystals with heavier halide (Figure S7). The effect of magnetic field (10 T) on PL dynamics of $CsPbBr_3$ nanocrystals is similar to that observed by Canneson et al. with a field of 10 T.[34] The

DOI: 10.1021/acs.nanolett.8b00184
Nano Lett. 2018, 18, 2074−2080

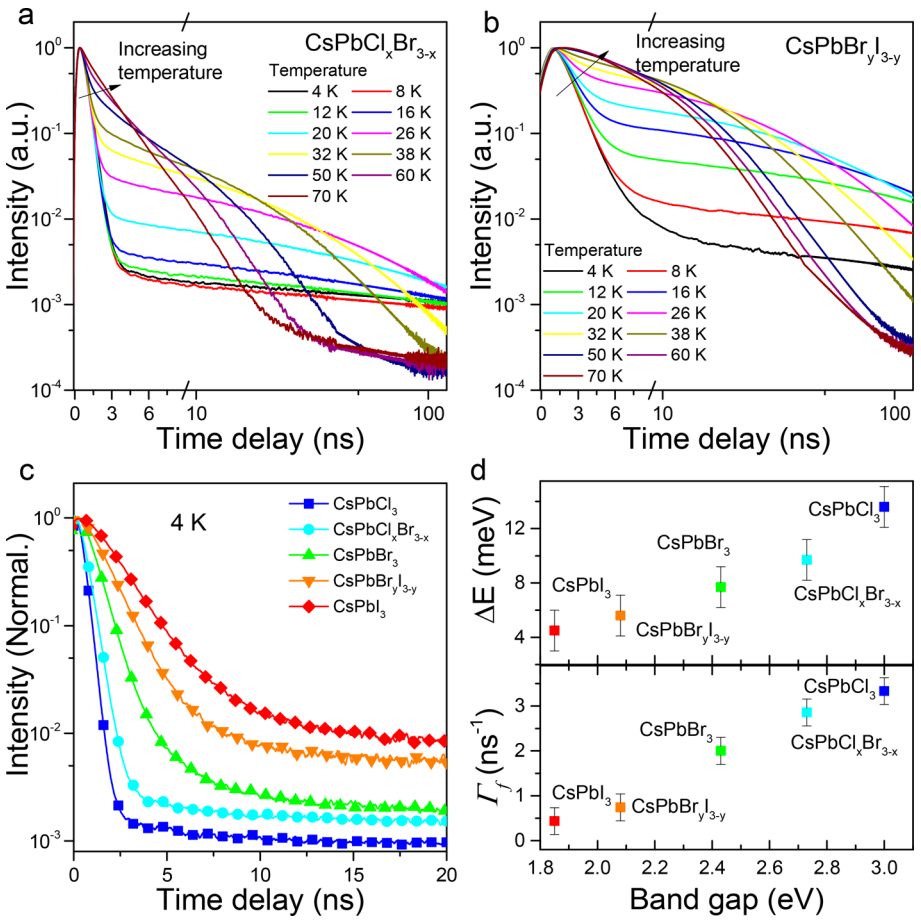

Figure 3. Temperature-dependent PL dynamics of (a) $CsPbCl_xBr_{3-x}$ and (b) $CsPbBr_yI_{3-y}$ nanocrystals, respectively. (c) Early-stage dynamics of PL emission from $CsPbX_3$ nanocrystals with different halide compositions. (d) Halide composition dependence of the derived energy splitting (ΔE) and the decay rate of the fast component (Γ_f). The values are plotted vs the band gaps of different nanocrystals at room temperature.

magnetic field effect is relatively small as an evidence of large ΔE with respect to the Zeeman energy.[37] When ΔE decreases, the effect of magnetic field becomes much more significant in $CsPbI_3$ nanocrystals. These results agree well with the scenario of magnetic field induced mixing of bright and dark states. We plot ΔE as a function of the band gap of $CsPbX_3$ nanocrystals in Figure 3d. The dependences on the halide are similar for ΔE and Γ_f (Figure 3d).

We discuss the possible mechanism responsible for the dependence of dark exciton dynamics on the halide. Generally, the dark state in semiconductor nanocrystals has been theoretically considered to originate from the spin configuration of electrons and holes,[34,36,37] where ΔE is mainly induced by the electron−hole exchange interaction. At 4 K, the fast component of PL dynamics may be contributed by the recombination of excitons, charged excitons, or both.[31,32,34] In semiconductor nanocrystals, the rate of charged exciton recombination is proportional to that of interband recombination of neutral exciton.[31,58] The magnitudes of both the exchange interaction and the oscillator strength of excitonic transitions are primarily determined by the overlap of electron and hole wave function,[53,59] which explains the similar dependences of ΔE and Γ_f on the halide (Figure 3d). The quantum size effect is also important in nanocrystals. In the strong confinement regime, ΔE is scaled as $\Delta E \approx V_0/L^3$, where V_0 is the volume of the unit cell;[36,53] In the weakly confinement regime, $\Delta E \approx V_0/a_B{}^3$, where a_B is the excitonic Bohr radius.[36,53] The trend of halide dependence of ΔE can be qualitatively explained in the weak confinement regime, suggesting that quantum confinement effect has a relatively small influence on the optical properties of nanocrystals studied here. This result is consistent with the nanocrystal size L = 10 nm in this study, which is larger than Bohr radius of $CsPbCl_3$ (5 nm) and $CsPbBr_3$ (7 nm) and comparable to that of $CsPbI_3$ (12 nm),[5] suggesting that the quantum confinement in our samples is not as strong as that is reported in CdSe nanocrystals.[37,50] Moreover, the strength of the exchange interaction evaluated from single dot spectroscopy[33] is smaller than that estimated for ΔE here. Besides the sample diversity and possible errors related to the three-model model, such a discrepancy may be caused by the involvement of other factors such the Rashba effect,[32] structure distortion at low temperature,[31] or trion states;[31,34] future in-depth study is needed.

Very recently, Becker et al. have extended the three-level model by including the Rashba spin−orbital effect.[60] The triplet excitons are predicted to be bright and the dark state is possibly to be above the bright levels, which has succeeded in explaining the polarization dependence of PL emission from single nanocrystals.[34,60] Nevertheless, the long-lived component at 4 K observed here, which is sensitive to the magnetic field, cannot be explained if the dark level is above the bright levels (Figure S5).[34] Such a divergence is possibly related to the polymorph nature of perovskite semiconductor nanocrystals in different studies. As recently reviewed by Kovalenko et al.,[61] the crystal

DOI: 10.1021/acs.nanolett.8b00184
Nano Lett. 2018, 18, 2074−2080

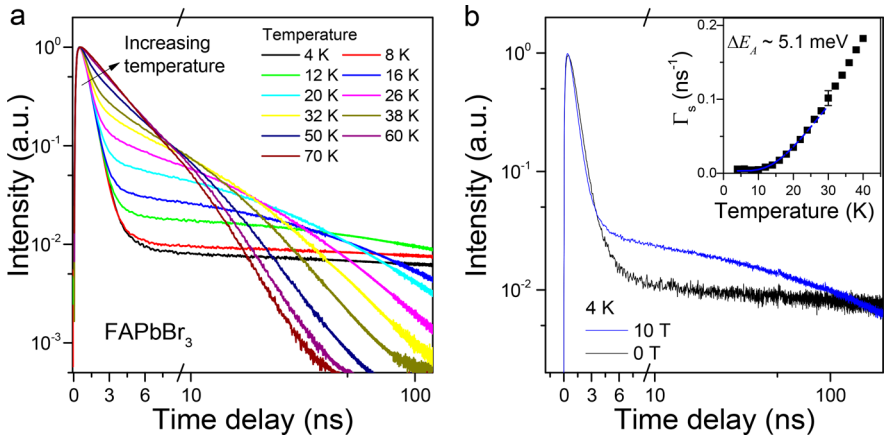

Figure 4. (a) Temperature-dependent PL dynamics in $FAPbBr_3$ nanocrystals. (b) PL dynamics of $FAPbBr_3$ nanocrystals recorded at 4 K with and without an applied magnetic field of 10 T. Inset shows the temperature-dependent decay rate of the slow component.

structures of perovskite semiconductors are susceptible to the surface and defects, which may cause different relative stabilities of various polymorphs. The nanocrystals with different crystal structures may be synthesized in a same batch of samples.[61] For instance, Fu et al. have shown that there are at least two different structures for $CsPbBr_3$ samples at low temperature.[31] Even in a single sample, twin subdomains have been observed, which may result in a higher-symmetry structure on average.[62] Rashba effect is strongly dependent on the structure asymmetry. The modification in energy structure caused by Rashba effect in different samples may be different due to different degree of structure distortion.[32] In samples with weak Rashba effects, the dark level could be lower than the bright levels, as observed in ref 34 and this work, while the energy level of some other nanocrystal samples with strong Rashba effect may fit well with the newly proposed model.[60] The presence of a long-lived excited state in some nanocrystals is further confirmed by TA spectroscopic measurements (Figure S9). In the TA trace, over 20% amplitude ratio of the long-lived component is clearly observed at cryogenic temperatures (Figure S9b), which is consistent with the presence of dark states (see the Supporting Information for more details).

Besides the halide at the X site, the cation at the A site also affects the exciton properties. Organic cations at X sites have been regarded as a critical factor influencing the optoelectronic performance of perovskite semiconductors.[44] Although the major features of valence and conduction bands originate from the inorganic sub lattice (PbX_3^-), the fast motion of dipolar organic cations may strongly affect the dynamics of charge carriers.[43,45] Of particular interest is the formation of large polarons, which may screen the Coulomb potential for charge carriers.[47,63] We compare the PL dynamics of $CsPbBr_3$ and $FAPbBr_3$ nanocrystals of similar sizes to study the effect of cations on dark exciton dynamics. The a_B of $FAPbBr_3$ (8 nm) is also similar to that of $CsPbBr_3$,[22] so the size effect can be safely excluded. Figure 4 shows TRPL curves measured from $FAPbBr_3$ nanocrystals. In comparison to $CsPbBr_3$ nanocrystals (Figure 2), the slow component is more important in $FAPbBr_3$ nanocrystals than that in $CsPbBr_3$ nanocrystals (Figure 4a), and the magnetic field effect is larger (Figure 4b). These results suggest the dark state plays a more important role in $FAPbBr_3$ nanocrystals, which is consistent with the smaller ΔE in $FAPbBr_3$ nanocrystals as confirmed by analyzing the temperature-dependent results (see the inset of Figure 4b). Such a difference can be ascribed to the screening effect in perovskite semiconductors with organic cations. The dielectric constant of $FAPbBr_3$ (~20) is much larger than that of $CsPbBr_3$ (~5).[5,22] The large charge screening effect will weaken the exchange interaction, leading to the observed smaller ΔE in $FAPbBr_3$ nanocrystals. A similar result has also been observed in $MAPbBr_3$ nanocrystals (Figure S8), confirming the critical role of carrier screening in perovskite semiconductor nanocrystals with organic cations. This might be a factor causing the efficiency improvement of $CsPbBr_3$ LEDs upon incorporation of MA organic cations.[20]

In summary, we have studied the dynamics of dark excitons in perovskite semiconductor nanocrystals with different compositions. The dark state is intrinsic to all perovskite semiconductor nanocrystals with different anions, cations, or both. ΔE is susceptible to the halide and organic cations, suggesting that it is possible to manipulate the dark exciton dynamics in perovskite nanocrystals by composition engineering. These findings will be instrumental in the design of LEDs and quantum light emitters with high performance.

■ ASSOCIATED CONTENT

Supporting Information

The Supporting Information is available free of charge on the ACS Publications website at DOI: 10.1021/acs.nanolett.8b00184.

Experimental details, sample characterization of $FAPbBr_3$ nanocrystals, additional data on PL dynamics of $CsPbBr_3$ nanocrystals, solution of three-level model and simulation results, fitting details, examples and table of fitting parameters, magnetic field effect of different halides, results from $MAPbBr_3$ nanocrystals, TA spectroscopic data, and data plotted in short and long time windows for clarity. Figures showing TEM images, TRPL curves, amplitudes, time-resolved PL spectra, a simulation of PL dynamics, decay and relaxation rates, and a time-resolved trace. Tables showing the fitting parameters of decay and spin-flip rates and energy splitting. (PDF)

■ AUTHOR INFORMATION

Corresponding Authors

*E-mail: cfzhang@nju.edu.cn. Telephone: +86-25-83621391.
*E-mail: mxiao@uark.edu. Telephone: +01-479-575-6568.

DOI: 10.1021/acs.nanolett.8b00184
Nano Lett. 2018, 18, 2074−2080

ORCID

Chunfeng Zhang: 0000-0001-9030-5606

Notes

The authors declare no competing financial interest.

■ ACKNOWLEDGMENTS

This work is supported by the National Key R&D Program of China (grant nos. 2017YFA0303703 and 2013CB932903), the National Science Foundation of China (grant nos. 11574140, 91233103, and 11621091), Jiangsu Provincial Funds for Distinguished Young Scientists (grant no. BK20160019).The authors acknowledge Dr. Xuewei Wu for his technical assistance.

■ REFERENCES

(1) Kojima, A.; Teshima, K.; Shirai, Y.; Miyasaka, T. *J. Am. Chem. Soc.* **2009**, *131*, 6050.
(2) Im, J.-H.; Lee, C.-R.; Lee, J.-W.; Park, S.-W.; Park, N.-G. *Nanoscale* **2011**, *3*, 4088.
(3) Kim, H.-S.; Lee, C.-R.; Im, J.-H.; Lee, K.-B.; Moehl, T.; Marchioro, A.; Moon, S.-J.; Humphry-Baker, R.; Yum, J.-H.; Moser, J. E.; Graetzel, M.; Park, N.-G. *Sci. Rep.* **2012**, *2*, 591.
(4) Lee, M. M.; Teuscher, J.; Miyasaka, T.; Murakami, T. N.; Snaith, H. J. *Science* **2012**, *338*, 643.
(5) Protesescu, L.; Yakunin, S.; Bodnarchuk, M. I.; Krieg, F.; Caputo, R.; Hendon, C. H.; Yang, R. X.; Walsh, A.; Kovalenko, M. V. *Nano Lett.* **2015**, *15*, 3692.
(6) Zhang, F.; Zhong, H.; Chen, C.; Wu, X.; Hu, X.; Huang, H.; Han, J.; Zou, B.; Dong, Y. *ACS Nano* **2015**, *9*, 4533.
(7) Protesescu, L.; Yakunin, S.; Bodnarchuk, M. I.; Bertolotti, F.; Masciocchi, N.; Guagliardi, A.; Kovalenko, M. V. *J. Am. Chem. Soc.* **2016**, *138*, 14202.
(8) Luo, B.; Pu, Y.-C.; Lindley, S. A.; Yang, Y.; Lu, L.; Li, Y.; Li, X.; Zhang, J. Z. *Angew. Chem., Int. Ed.* **2016**, *55*, 8864.
(9) Swarnkar, A.; Chulliyil, R.; Ravi, V. K.; Irfanullah, M.; Chowdhury, A.; Nag, A. *Angew. Chem., Int. Ed.* **2015**, *54*, 15424.
(10) Tong, Y.; Bladt, E.; Aygueler, M. F.; Manzi, A.; Milowska, K. Z.; Hintermayr, V. A.; Docampo, P.; Bals, S.; Urban, A. S.; Polavarapu, L.; Feldmann, J. *Angew. Chem., Int. Ed.* **2016**, *55*, 13887.
(11) Bekenstein, Y.; Koscher, B. A.; Eaton, S. W.; Yang, P.; Alivisatos, A. P. *J. Am. Chem. Soc.* **2015**, *137*, 16008.
(12) Akkerman, Q. A.; Motti, S. G.; Kandada, A. R. S.; Mosconi, E.; D'Innocenzo, V.; Bertoni, G.; Marras, S.; Kamino, B. A.; Miranda, L.; De Angelis, F.; Petrozza, A.; Prato, M.; Manna, L. *J. Am. Chem. Soc.* **2016**, *138*, 1010.
(13) Zhang, X.; Lin, H.; Huang, H.; Reckmeier, C.; Zhang, Y.; Choy, W. C.; Rogach, A. L. *Nano Lett.* **2016**, *16*, 1415.
(14) Zhang, X.; Sun, C.; Zhang, Y.; Wu, H.; Ji, C.; Chuai, Y.; Wang, P.; Wen, S.; Zhang, C.; Yu, W. W. *J. Phys. Chem. Lett.* **2016**, *7*, 4602.
(15) Xing, J.; Yan, F.; Zhao, Y.; Chen, S.; Yu, H.; Zhang, Q.; Zeng, R.; Demir, H. V.; Sun, X.; Huan, A.; Xiong, Q. *ACS Nano* **2016**, *10*, 6623.
(16) Deng, W.; Xu, X.; Zhang, X.; Zhang, Y.; Jin, X.; Wang, L.; Lee, S.-T.; Jie, J. *Adv. Funct. Mater.* **2016**, *26*, 4797.
(17) Zhang, X. L.; Xu, B.; Zhang, J. B.; Gao, Y.; Zheng, Y. J.; Wang, K.; Sun, X. W. *Adv. Funct. Mater.* **2016**, *26*, 4595.
(18) Ling, Y.; Yuan, Z.; Tian, Y.; Wang, X.; Wang, J. C.; Xin, Y.; Hanson, K.; Ma, B.; Gao, H. *Adv. Mater.* **2016**, *28*, 305.
(19) Song, J.; Li, J.; Li, X.; Xu, L.; Dong, Y.; Zeng, H. *Adv. Mater.* **2015**, *27*, 7162.
(20) Zhang, L. Q.; Yang, X. L.; Jiang, Q.; Wang, P. Y.; Yin, Z. G.; Zhang, X. W.; Tan, H. R.; Yang, Y.; Wei, M. Y.; Sutherland, B. R.; Sargent, E. H.; You, J. B. *Nat. Commun.* **2017**, *8*, 15640.
(21) Stranks, S. D.; Snaith, H. J. *Nat. Nanotechnol.* **2015**, *10*, 391.
(22) Perumal, A.; Shendre, S.; Li, M.; Tay, Y. K. E.; Sharma, V. K.; Chen, S.; Wei, Z.; Liu, Q.; Gao, Y.; Buenconsejo, P. J. S.; et al. *Sci. Rep.* **2016**, *6*, 36733.
(23) Veldhuis, S. A.; Boix, P. P.; Yantara, N.; Li, M.; Sum, T. C.; Mathews, N.; Mhaisalkar, S. G. *Adv. Mater.* **2016**, *28*, 6804.
(24) Wang, Y.; Li, X.; Song, J.; Xiao, L.; Zeng, H.; Sun, H. *Adv. Mater.* **2015**, *27*, 7101.
(25) Xu, Y.; Chen, Q.; Zhang, C.; Wang, R.; Wu, H.; Zhang, X.; Xing, G.; Yu, W. W.; Wang, X.; Zhang, Y.; Xiao, M. *J. Am. Chem. Soc.* **2016**, *138*, 3761.
(26) Yakunin, S.; Protesescu, L.; Krieg, F.; Bodnarchuk, M. I.; Nedelcu, G.; Humer, M.; De Luca, G.; Fiebig, M.; Heiss, W.; Kovalenko, M. V. *Nat. Commun.* **2015**, *6*, 8056.
(27) Hu, F.; Zhang, H.; Sun, C.; Yin, C.; Lv, B.; Zhang, C.; Yu, W. W.; Wang, X.; Zhang, Y.; Xiao, M. *ACS Nano* **2015**, *9*, 12410.
(28) Rainò, G.; Nedelcu, G.; Protesescu, L.; Bodnarchuk, M. I.; Kovalenko, M. V.; Mahrt, R. F.; Stöferle, T. *ACS Nano* **2016**, *10*, 2485.
(29) Park, Y.-S.; Guo, S.; Makarov, N. S.; Klimov, V. I. *ACS Nano* **2015**, *9*, 10386.
(30) Hu, F.; Yin, C.; Zhang, H.; Sun, C.; Yu, W. W.; Zhang, C.; Wang, X.; Zhang, Y.; Xiao, M. *Nano Lett.* **2016**, *16*, 6425.
(31) Fu, M.; Tamarat, P.; Huang, H.; Even, J.; Rogach, A. L.; Lounis, B. *Nano Lett.* **2017**, *17*, 2895.
(32) Isarov, M.; Tan, L. Z.; Bodnarchuk, M. I.; Kovalenko, M. V.; Rappe, A. M.; Lifshitz, E. *Nano Lett.* **2017**, *17*, 5020.
(33) Yin, C.; Chen, L.; Song, N.; Lv, Y.; Hu, F.; Sun, C.; Yu, W. W.; Zhang, C.; Wang, X.; Zhang, Y.; Xiao, M. *Phys. Rev. Lett.* **2017**, *119*, 026401.
(34) Canneson, D.; Shornikova, E. V.; Yakovlev, D. R.; Rogge, T.; Mitioglu, A. A.; Ballottin, M. V.; Christianen, P. C.; Lhuillier, E.; Bayer, M.; Biadala, L. *Nano Lett.* **2017**, *17*, 6177.
(35) Labeau, O.; Tamarat, P.; Lounis, B. *Phys. Rev. Lett.* **2003**, *90*, 257404.
(36) Efros, A. L.; Rosen, M.; Kuno, M.; Nirmal, M.; Norris, D. J.; Bawendi, M. *Phys. Rev. B: Condens. Matter Mater. Phys.* **1996**, *54*, 4843.
(37) Nirmal, M.; Norris, D. J.; Kuno, M.; Bawendi, M. G.; Efros, A. L.; Rosen, M. *Phys. Rev. Lett.* **1995**, *75*, 3728.
(38) Akkerman, Q. A.; D'Innocenzo, V.; Accornero, S.; Scarpellini, A.; Petrozza, A.; Prato, M.; Manna, L. *J. Am. Chem. Soc.* **2015**, *137*, 10276.
(39) Hoffman, J. B.; Schleper, A. L.; Kamat, P. V. *J. Am. Chem. Soc.* **2016**, *138*, 8603.
(40) Parobek, D.; Dong, Y.; Qiao, T.; Rossi, D.; Son, D. H. *J. Am. Chem. Soc.* **2017**, *139*, 4358.
(41) Zhang, D.; Yang, Y.; Bekenstein, Y.; Yu, Y.; Gibson, N. A.; Wong, A. B.; Eaton, S. W.; Kornienko, N.; Kong, Q.; Lai, M.; Alivisatos, A. P.; Leone, S. R.; Yang, P. *J. Am. Chem. Soc.* **2016**, *138*, 7236.
(42) Nedelcu, G.; Protesescu, L.; Yakunin, S.; Bodnarchuk, M. I.; Grotevent, M. J.; Kovalenko, M. V. *Nano Lett.* **2015**, *15*, 5635.
(43) Motta, C.; El-Mellouhi, F.; Kais, S.; Tabet, N.; Alharbi, F.; Sanvito, S. *Nat. Commun.* **2015**, *6*, 7026.
(44) Frost, J. M.; Walsh, A. *Acc. Chem. Res.* **2016**, *49*, 528.
(45) Bakulin, A. A.; Selig, O.; Bakker, H. J.; Rezus, Y. L. A.; Mueller, C.; Glaser, T.; Lovrincic, R.; Sun, Z.; Chen, Z.; Walsh, A.; Frost, J. M.; Jansen, T. L. C. *J. Phys. Chem. Lett.* **2015**, *6*, 3663.
(46) Etienne, T.; Mosconi, E.; De Angelis, F. *J. Phys. Chem. Lett.* **2016**, *7*, 1638.
(47) Zhu, X. Y.; Podzorov, V. *J. Phys. Chem. Lett.* **2015**, *6*, 4758.
(48) Zhu, H.; Miyata, K.; Fu, Y.; Wang, J.; Joshi, P. P.; Niesner, D.; Williams, K. W.; Jin, S.; Zhu, X. Y. *Science* **2016**, *353*, 1409.
(49) Biadala, L.; Liu, F.; Tessier, M. D.; Yakovlev, D. R.; Dubertret, B.; Bayer, M. *Nano Lett.* **2014**, *14*, 1134.
(50) Labeau, O.; Tamarat, P.; Lounis, B. *Phys. Rev. Lett.* **2003**, *90*, 257404.
(51) Chirvony, V. S.; González-Carrero, S.; Suarez, I.; Galian, R. E.; Sessolo, M.; Bolink, H. J.; Martinez-Pastor, J. P.; Pérez-Prieto, J. *J. Phys. Chem. C* **2017**, *121*, 13381.
(52) Biadala, L.; Louyer, Y.; Tamarat, P.; Lounis, B. *Phys. Rev. Lett.* **2009**, *103*, 037404.
(53) Takagahara, T. *Phys. Rev. B: Condens. Matter Mater. Phys.* **1993**, *47*, 4569.

DOI: 10.1021/acs.nanolett.8b00184
Nano Lett. 2018, 18, 2074−2080

(54) Le Thomas, N.; Herz, E.; Schöps, O.; Woggon, U.; Artemyev, M. V. *Phys. Rev. Lett.* **2005**, *94*, 016803.
(55) de Mello Donegá, C.; Bode, M.; Meijerink, A. *Phys. Rev. B: Condens. Matter Mater. Phys.* **2006**, *74*, 085320.
(56) Zheng, F.; Tan, L. Z.; Liu, S.; Rappe, A. M. *Nano Lett.* **2015**, *15*, 7794.
(57) Narvaez, G. A.; Bester, G.; Franceschetti, A.; Zunger, A. *Phys. Rev. B: Condens. Matter Mater. Phys.* **2006**, *74*, 205422.
(58) Galland, C.; Ghosh, Y.; Steinbrueck, A.; Hollingsworth, J. A.; Htoon, H.; Klimov, V. I. *Nat. Commun.* **2012**, *3*, 908.
(59) Norris, D. J.; Efros, A. L.; Rosen, M.; Bawendi, M. G. *Phys. Rev. B: Condens. Matter Mater. Phys.* **1996**, *53*, 16347.
(60) Becker, M. A.; Vaxenburg, R.; Nedelcu, G.; Sercel, P. C.; Shabaev, A.; Mehl, M. J.; Michopoulos, J. G.; Lambrakos, S. G.; Bernstein, N.; Lyons, J. L.; Stöferle, T.; Mahrt, R. F.; Kovalenko, M. V.; Norris, D. J.; Rainò, G.; Efros, A. L. *Nature* **2018**, *553*, 189.
(61) Kovalenko, M. V.; Protesescu, L.; Bodnarchuk, M. I. *Science* **2017**, *358*, 745.
(62) Bertolotti, F.; Protesescu, L.; Kovalenko, M. V.; Yakunin, S.; Cervellino, A.; Billinge, S. J. L.; Terban, M. W.; Pedersen, J. S.; Masciocchi, N.; Guagliardi, A. *ACS Nano* **2017**, *11*, 3819.
(63) Zhu, H.; Miyata, K.; Fu, Y.; Wang, J.; Joshi, P. P.; Niesner, D.; Williams, K. W.; Jin, S.; Zhu, X.-Y. *Science* **2016**, *353*, 1409.

DOI: 10.1021/acs.nanolett.8b00184
Nano Lett. 2018, 18, 2074−2080